DOI: 10.1002/ejic.201100795

Concentration-Dependent Dehydrogenation of Ammonia–Borane/Triglyme Mixtures

Johannes F. Kostka,[a] René Schellenberg,[b] Felix Baitalow,[b] Tom Smolinka,[a] and Florian Mertens*[b]

Keywords: Ammonia borane / Dehydrogenation / Hydrogen storage / Kinetics / Reaction mechanisms / Thermolysis

The dehydrogenation reaction of the hydrogen-storage compound ammonia–borane (AB) dissolved in triglyme (TG) reveals an unexpected but favourable concentration dependence of its dehydrogenation behaviour. Formal reaction-order considerations and ^{11}B NMR spectroscopic analytics point towards a complex AB decomposition and hydrogen-release scheme that in highly concentrated solutions partly begins to resemble that of the solid-state case. The analysis of the gas-release characteristics identified two hydrogen desorption events that display an increasing peak overlap with increasing initial AB concentration. ^{11}B NMR spectroscopic studies indicate that the concentration-dependent stability of the intermediate diammoniate of diborane, the presence of which appears to influence the rates of several dehydrogenation steps by interacting with various other intermediates, is one of the key factors for the overall hydrogen release.

Introduction

Ammonia–borane (AB) is regarded as a promising candidate to fulfil the requirements for a high-density and easy-to-handle hydrogen source material.[1] With its high hydrogen content of 19 wt.-% and a release of 13.5 wt.-% at temperatures below 140 °C,[1,2] it possesses outstanding qualities for this application. In this respect, one important obstacle to using pure AB is given by its poor dehydrogenation kinetics, which would limit its use to applications with a high energy-demand-to-power ratio. To achieve the necessary improvements in dehydrogenation kinetics, a detailed understanding of structure, hydrogenation/dehydrogenation mechanisms and their rate-limiting steps is imperative and have been the subject of a significant number of studies during the past decade.[1–5]

Consistent with earlier findings that the thermally induced dehydrogenation reaction of solid AB has an induction period, recent investigations show that the dehydrogenation of solid AB may be characterized by a nucleation and growth process.[3] After the induction period, the release seems to follow a two-step scheme.[2] The first release step has its onset at about 120 °C, which is just above the melting point of AB.[2] These findings suggest a kinetic enhancement for the dehydrogenation due to the presence of mobile phases.

In a recent publication,[3] thermal decomposition of solid AB was found to be initiated by a species AB*, which is assumed to be mobile. Thereafter, two mobile AB* units may form the intermediate called diammoniate of diborane $[BH_2(NH_3)_2]^+[BH_4]^-$ (DADB), which is regarded as a nucleus for the dehydrogenation reaction. Once formed, or externally added to pure AB, DADB seems to promote the dehydrogenation kinetics significantly.[3] The kinetics of this reaction were also substantially enhanced in ionic liquids (e.g., bmimCl, in which bmim = 1-butyl-3-methylimidazolium).[4] Here, too, DADB was described as an intermediate.[4] From their recent work on AB in diglyme, Autrey et al.[6] reported on possible traces of DADB in a 2 M solution at 50 °C. From these results they concluded that DADB in solutions requires stabilization by a polar environment.[4,6]

Hence, controlling the DADB formation by the means of the reaction environment could enhance the mobility of AB and seems to be a promising approach to improve the dehydrogenation kinetics. For high gravimetric hydrogen densities in the storage medium, however, the weight fraction of the reaction environment (e.g., the solvents or catalysts) and the chemical performance has to be optimized.

In this paper, the findings of significant amounts of DADB in highly concentrated solutions of AB in the weakly polar solvent triglyme (TG) and its positive consequences for the dehydrogenation kinetics of AB and the possible underlying reaction pathways will be discussed. For this purpose, we combined the method of gas volumetric measurements with ex situ ^{11}B NMR spectroscopy.

---

[a] Fraunhofer Institute for Solar Energy Systems, Dept. Energy Technology
Heidenhofstrasse 2, 79110 Freiburg, Germany
Fax: +49-761-4588-9320
E-mail: johannes.kostka@ise.fraunhofer.de
[b] Technische Universität Bergakademie Freiberg, Fakultät für Chemie und Physik
Leipziger Strasse 29, 09599 Freiberg, Germany
Fax: +49-3731-39-35-88
E-mail: Florian.Mertens@chemie.tu-freiberg.de

Results and Discussion

Dehydrogenation Kinetics

Dehydrogenation characteristics of the thermolysis reaction (at T = 70 °C) were investigated over a wide range of concentrations, from dilute solutions of $[AB]_0 = 0.1$ M up to suspensions of $[AB]_0 = 23.0$ M (Figure 1a). The time needed to release 1 mol of H_2 per mol of AB [$t_{1/2}(H_2)$] as a function of the initial AB concentration ($[AB]_0$) decays asymptotically to (40 ± 10) min at the saturation concentration $[AB]_0 \approx [AB]_{sat} = 7.5$ M and rises again for concentrations $[AB]_0 \geq 9.0$ M (suspensions). Experiments with concentrations well above $[AB]_{sat}$ show nucleation and growth characteristics that are typical of solid AB according to the literature[3] (see Figure 1). Hence, the best dehydrogenation kinetics are achieved in highly concentrated AB solutions. Therefore, the work presented will only focus on systems with AB in solution.

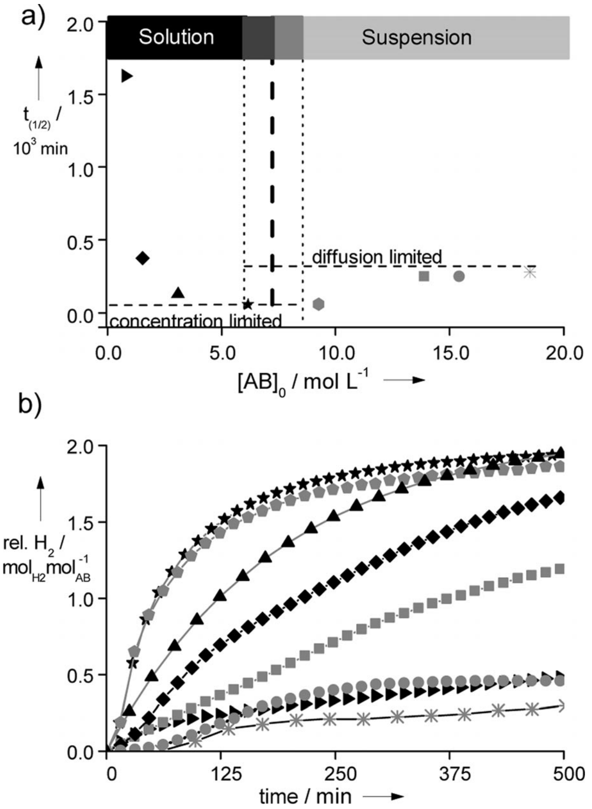

Figure 1. Hydrogen-release characteristics of AB in TG at T = 70 °C for mixtures with concentrations between 1.5 and 18 M. (a) Plot of the half-time of the total hydrogen release (i.e., the equivalent of 1 mol of H_2 per mol of BH_3NH_3 versus the concentration of the initial AB concentration in TG. (b) Amount of hydrogen released as a function of time given in mol H_2 per mol BH_3NH_3.

In a first step to determine the kinetics of the dehydrogenation reaction, the emitted gas volume was characterized by a plot of the time required to release 0.5, 1.0 and 1.5 mol H_2 per mol of AB ($t_{1/4}$, $t_{1/2}$ and $t_{3/4}$, respectively) as a function of $[AB]_0^{-1}$ (Figure 2a) and $[AB]_0^{-2}$ (Figure 2b). For the early dehydrogenation phase, a linear dependence of $t_{x = 1/4}(H_2)$ on $[AB]_0^{-1}$ can be estimated, which would correspond to a second-order kinetics (see Figure 2a). In contrast, the kinetics of the later dehydrogenation phase are better characterized by a linear dependence of $t_{1/2}(H_2)$ and $t_{3/4}(H_2)$ on $[AB]_0^{-2}$, which would correspond to a formal third-order rate law for the formation of H_2 as a function of $[AB]_0$ (see Figure 2b).

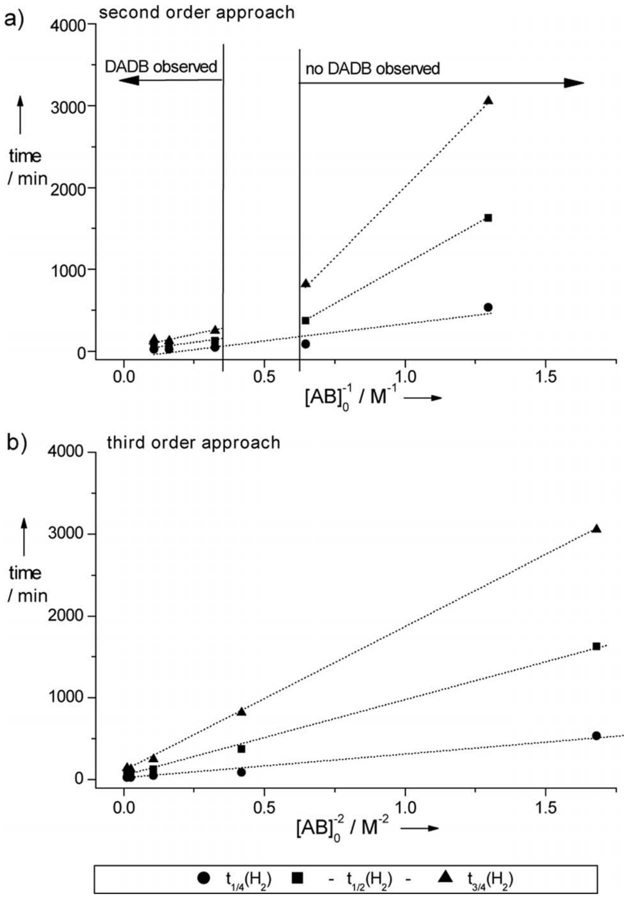

Figure 2. Time elapsed until the release of 0.5, 1.0 and 1.5 mol-equiv. of H_2 [$t_{x = 1/4,\, 1/2,\, 3/4}(H_2)$] at T = 70 °C plotted versus (a) $[AB]_0^{-1}$ (a distinct deviation from a second-order behaviour is observed for $t_{x \geq 1/2}$) and (b) $[AB]_0^{-2}$ (as a test for third-order kinetics).

The simple assumption that one third-order reaction is governing the dehydrogenation process appears to be very unlikely if one takes into account that AB decomposes in glymes according to a second-order rate law with respect to the AB concentration.[6] In addition, calculations of the rate constants according to a third-order law do not result in a single value for all curves in Figure 2b, thus indicating that this rate law also does not apply.

One possible explanation for the aforementioned dehydrogenation behaviour can be extracted from the time derivative of the released hydrogen gas volume (see Figure 3). It can be seen that at least two distinct desorption events more strongly overlap with increasing $[AB]_0$ concentrations. The simultaneous occurrence of these two desorption events leads to an enhanced hydrogen development at higher concentrations during the early reaction phase (see Figure 2a, left-hand side).

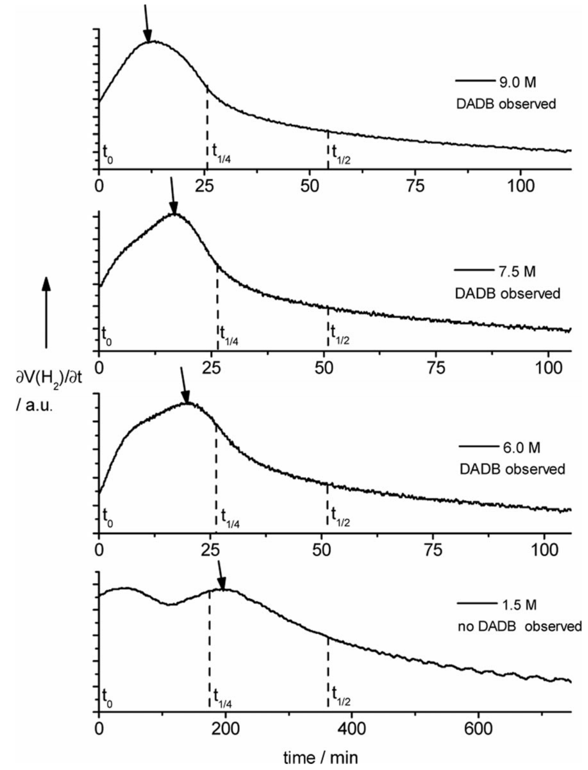

Figure 3. Time derivation of the gas volume of the hydrogen released at 70 °C from AB/TG solutions with different initial AB concentrations.

Moreover, the first event displays its maximum hydrogen flow significantly after t_0. Such behaviour indicates that the hydrogen release is not governed by a single elementary decomposition reaction of any order but needs to proceed through an intermediate compound.

To understand the underlying mechanistic steps responsible for such behaviour, we coupled the dehydrogenation experiments with ex situ ^{11}B NMR spectroscopy.

^{11}B NMR Spectroscopy of the Reaction Phase $t < t_{1/4}$

As stated above, during the early reaction phase, the dehydrogenation kinetics can be fit to a second-order law, which may be satisfactorily explained by the bimolecular reaction of two AB molecules to DADB with a subsequent cyclization to cyclodiborazane (CDB, c-$B_2N_2H_8$) under the release of 1 mol-equiv. H_2 (see Scheme 1). Such a mechanism was recently proposed for AB/glyme mixtures by Autrey et al. but could not yet be confirmed since the authors found only traces of DADB at low reaction temperatures.

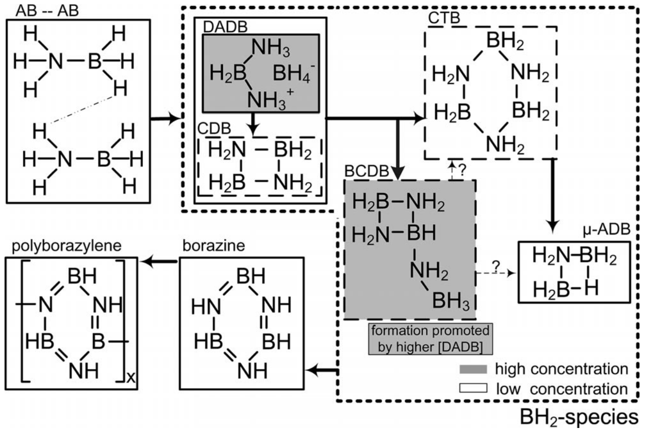

Scheme 1. Proposed dehydrogenation pathways of AB in TG at 70 °C based on NMR spectroscopy. Solid boxes denote unambiguous observed signals; dashed boxes indicate proposed species based on results of Shaw et al.;[6] dotted boxes frame BH_2 species. DADB was observed only at $[AB]_0 > 1.5$ M but seems to promote the formation of *B*-(cyclodiborazanyl)aminoborohydride (BCDB).

Our ^{11}B NMR spectra of the early reaction of dilute solutions ($[AB]_0 < 1.5$ M) also show only two significant resonances. Beside the prominent AB-related quintet at δ = –21.5 ppm, a signal at δ = –10.5 ppm is observed, which is assigned to CDB according to other publications (see Table 1).[6,7]

For highly concentrated solutions ($[AB]_0 > 1.5$ M), we observe an additional quintet resonance at δ = (–36.5 ± 0.5) ppm (see Figure 4a), which can be assigned to DADB.[3,4] This assignment is also supported by the correlation with the signal of the BH_2 group at δ = –10.7 ppm. Because various components {CDB, cyclotriborazane (c-$B_3N_3H_{12}$, CTB), *B*-(cyclodiborazanyl)aminoborohydride

Table 1. Assignment of ^{11}B NMR spectroscopic signals to the relevant species found during AB/TG dehydrogenation experiments.

Species	^{11}B (20 °C)[a] [ppm]	$^1J_{B,H}$ [Hz]	Referenced literature
DABD	(–36.5 ± 0.5) (BH_4)[b]	79 (quint)	[3,6]
AB	–21.5 (BH_3)	78 (quint)	[6,7]
μ-ADB	–26.5 (H-N-BH_2)	56 (d), 113 (t)	[7,9]
BCDB	–4.5 (NH_2BH_3)	[c]	[6]
CTB, CDB, BCDB	–10 to –13 (BH_2)	[c]	[3,4,6]
Boroxide (traces)	1.5 (BO)	–	–
Polyborazylene	25.0 $(BHNH)_x(BH_2)_x(BH_3)_x$[d]	–	[4,6]
Borazine	30.5 $(HNBH)_3$[d]	113 (d)	[3,4,6,7]

[a] ^{11}B chemical shifts are referenced to the IUPAC standard $BF_3 \cdot OEt_2$ (δ = 0 ppm) at 20 °C. [b] Species only found in samples $[AB] > 1.5$ M. [c] No multiplets observable. [d] $[AB] < 18$ M.

(*cyc*[$NH_2BH_2NH_2BH$]-NH_2BH_3, BCDB)} also contribute to this signal, it is not correlated with the DADB signal at δ = –36.5 ppm and thus does not follow its decrease with the progress of the dehydrogenation reaction. Our findings in highly concentrated solutions strongly support Autrey and co-workers'[6] assumption that the AB decomposition proceeds by means of the formation of DADB and CDB to CTB. Because our resolution of the δ = –10.7 ppm peak is not sufficient, it is not evident whether or not CDB forms after or simultaneously with DADB.

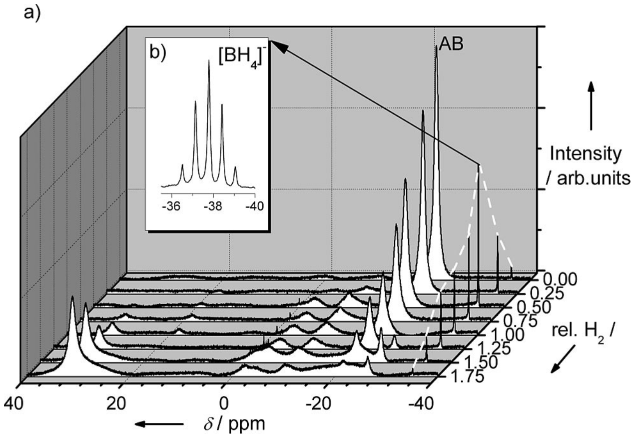

Figure 4. (a) $^{11}B\{^1H\}$ NMR spectra depicting the dehydrogenation evolution form an AB/TG solution ($[AB]_0$ = 6.0 M) at 70 °C. (b) The quintet signal at $\delta \approx (-36.5 \pm 0.5)$ ppm in the coupled spectra is identified as the BH_4 resonance of DADB and can be traced almost along the whole dehydrogenation process.

Although it cannot be stated for diluted solutions ($[AB]_0 \leq 1.5$ M) whether or not the absence of DADB-related signals is due to DADB concentrations that are below the detection limit, the observation, however, that the hydrogen release rate for $[AB]_0$ = 1.5 M reaches its maximum shortly after t_0 (see Figure 3) supports the assumption of the presence of an early intermediate, be it DADB or CDB.

During the early reaction phase $t < t_{1/4}$, the BH_2 signal at $\delta \approx$ –10.7 ppm grows and slightly shifts to δ = –10.0 ppm (see Figure 5). From DADB-enriched AB/TG solutions compared to pure AB/TG solutions, one has to assign the signal at δ = –10.7 ppm to the BH_2 group of DADB. Based on the experiments with the diluted solutions ($[AB]_0 \leq 1.5$ M), we assign the δ = –10.7 ppm signal to CDB as well. Together with the observation described in the literature[6] that the CTB-BH_2 signal is slightly shifted to lower absolute ppm values in respect to the CDB-BH_2 signal, we interpret the evolving peak at δ = –10.0 ppm as a result of the formation of CTB out of DADB and/or CDB.

Since the occurrence of the third-order decomposition law could not be simply derived from the early reaction mechanism, an analysis of the formation of intermediates by ^{11}B NMR spectroscopy was also performed for the reaction phase $t > t_{1/4}(H_2)$.

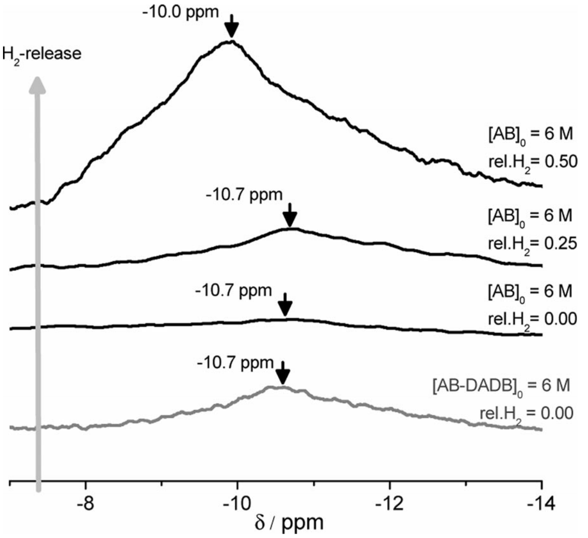

Figure 5. Excerpt of ^{11}B NMR spectra representing only BH_2 signals. All spectra are normalized by their integrals, representing the total boron content of each sample and thus allowing the direct comparison of the intensities. Grey: spectrum of a DADB-enriched AB/TG solution before dehydrogenation. Black: spectra of AB/TG solutions at different stages of dehydrogenation. The very shallow maximum at δ = –10.7 ppm at the beginning of the recording of the hydrogen evolution (rel. H_2 = 0) is most likely due to a minute hydrogen release that was not detected during the sample preparation.

^{11}B NMR Spectroscopy of the Reaction Phase $t > t_{1/2}$

By the determination of the relative peak area of the signal at $\delta \approx$ 30.5 ppm, we estimate that about (15 ± 2)% of the total boron content is bound in borazine in all samples with $[AB]_0 > 1.5$ M after the reaction has proceeded to $t_{1/2}(H_2)$ (see Figure 4).

Samples with lower concentrations in which no DADB was observed show significantly less borazine [about (5 ± 1)%] at this point of reaction. These findings suggest that the hydrogen release from these mixtures is 15% higher than would be expected from the reaction of AB through DABD to CDB alone.

The DADB-related signal peaks around $t_{1/4}$ with a relative peak area of (2 ± 1)% for $[AB]_0$ = 3.0 M and of (4 ± 1)% for $[AB]_0$ = 6.0 M. The correlation between the high DADB and the high borazine concentrations at $t_{1/2}$ suggests that DADB is linked to an accelerated decomposition to borazine and the accompanied hydrogen release.

Shortly after the rise of the DADB-related signal, a resonance at δ = –4.5 ppm occurs, the relative area of which also increases with increasing $[AB]_0$ concentrations (see Figure 6). We attribute this signal to the BNH_3 fragment of the recently identified BCDB.[6] The relative peak area of this signal at δ = –4.5 ppm follows a two-step pattern. Here, each step is followed by a short plateau (see Figure 6). The levels of these plateaus rise with increasing $[AB]_0$ concentrations. Prior to the onset of the second plateau, a sharp decline of the signal's relative area at $\delta \approx -10.5$ ppm is observable, which we attribute to BH_2 resonances and interpret as a transition from CDB[6,7] to BCDB.

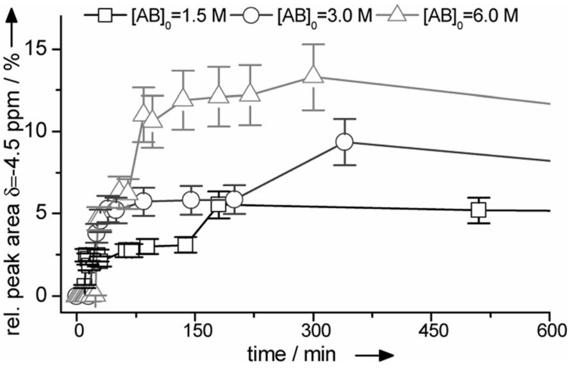

Figure 6. Analysis of the relative area of the BCDB-related peak at $\delta = -4.5$ ppm for different $[AB]_0$ values. The BCDB formation characteristics display two plateaus during the reaction. The relative peak areas rise with increasing $[AB]_0$.

Thus, in our measurements, higher $[AB]_0$ values seem to correlate with both higher [BCDB] and higher [DADB] ones. An apparent correlation between increased [DADB] and increased [BCDB] levels is supported by experiments we conducted with separately prepared mixtures of AB and DADB, which were prepared according to the procedure described by Shore et al.[8] During the significantly enhanced dehydrogenation process, a rise of the relative peak area at $\delta = -4.5$ ppm (BCDB) was observed (see Figure 7).

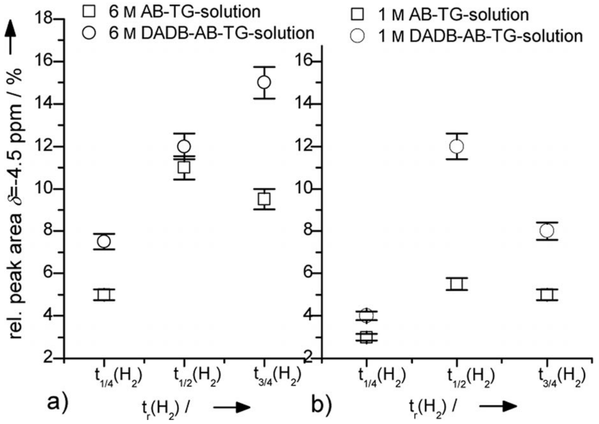

Figure 7. Evolution analysis of the relative areas of the BCDB-related ^{11}B NMR spectroscopic peak at $\delta = -4.5$ ppm for different $[AB]_0$ values during the dehydrogenation reaction of (a) 6.0 M and (b) 1.0 M solutions of AB/TG and AB/DADB/TG mixtures. The addition of DADB significantly promotes the formation of BCDB.

On the basis of experiments with separately prepared and heated CTB/TG samples, we ruled out the formation of BCDB from CTB, since we could not detect the $\delta = -4.5$ ppm signal, even at elevated temperatures (see Figure 8).

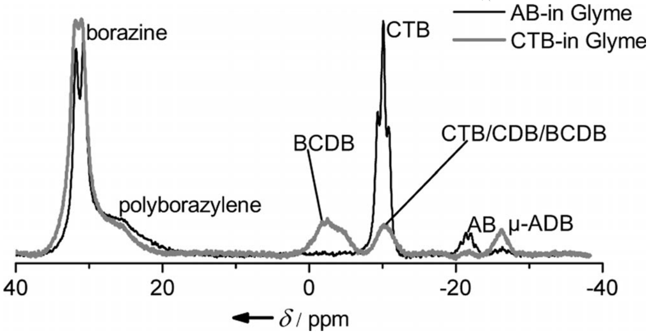

Figure 8. Coupled $^{11}B\{^1H\}$ NMR spectra[8] of samples of AB (black line) and CTB (grey line) in glyme, which were dehydrogenated at 90 and 130 °C for 4 h, respectively. The spectrum of CTB does not show any signal of BCDB or CDB, whereas highly concentrated AB/TG solutions react to form CDB, BCDB and significant amounts of µ-ADB.

Hence, we interpret the noticed acceleration of the formation of borazine from CDB through BCDB as being induced or promoted by the increased presence of DADB.

^{11}B NMR Spectroscopy of the Reaction Phase $t > t_{1/2}$

For the reaction phase $t > t_{1/2}$, the building of µ-aminodiborane (µ-ADB, µ-$[NH_2BH_5]$) seems to be another vital intermediate step to form borazine. The sextet signal at $\delta = -26.5$ ppm, which we assign to µ-ADB, shows up shortly after $t_{1/2}(H_2)$ and remains present until all hydrogen is released (see Figure 4). In the separately prepared CTB samples, µ-ADB is the only compound found beside borazine (see Figure 8).

The detected dehydrogenation of pure CTB/TG samples is significantly slower than in CDB- or BCDB-rich AB/TG samples with $[AB]_0 > 1.5$ M. Thus, we assume two alternative pathways to borazine: an early, fast one that occurs through BCDB and a late, slow one through µ-ADB. For diluted solutions, however, with $[AB]_0 < 1.0$ M both of these pathways seem, at least partially, to be blocked at 70 °C since neither DADB nor µ-ADB were detected.

In accordance with this interpretation, the measured hydrogen yield strongly deviates from the theoretical expected value of 2 mol H_2 per mol of AB. For example, for the initial concentrations of $[AB]_0 = 0.8$, 0.5 and 0.15 M, only 1.8, 1.5 and 0.3 mol H_2 per mol of AB were released, respectively.

Conclusion

We have found a concentration-dependent overlap of at least two distinct dehydrogenation events by gas kinetic analysis in AB/TG solutions. ^{11}B NMR spectroscopy demonstrates that the relative amounts both of DADB as well as of BCDB formed during thermal decomposition are increased in highly concentrated solutions. Moving from decomposition experiments with highly concentrated AB/TG solutions to the ones enriched with DADB, even higher relative amounts of BCDB are found. In addition, the presence of the latter compound appears to accelerate the formation of borazine (i.e., its formation is observed earlier and in higher amounts with respect to the relative amount of hydrogen released). If we recall that the borazine formation is accompanied by hydrogen emission, we can conclude that through the formation of BCDB, DADB is indirectly responsible for the observed accelerated hydrogen release by the earlier occurrence of the second desorption event. In this context, the observed experimental third-order law of the decomposition kinetics appears to be a consequence of a shift in the downstream reaction pathways.

As a consequence of above deduced relationship between the DADB and BCDB concentrations, the absence of detectable DADB in samples with $[AB]_0$ concentrations below 1.5 м indicates that the BCDB pathway for the conversion of CDB to borazine becomes less important. This could also explain the incomplete dehydrogenation in such samples at 70 °C.

The presence of DADB in highly concentrated solutions in a weakly polar organic solvent gives reason to reconsider the hypothesis that such an environment destabilizes the ion pair $[NH_3BH_2NH_3]^+[BH_4]^-$.[4,6] Either this hypothesis is untenable or strongly concentrated solutions of AB in glymes lead to an increasingly polar environment that stabilizes DADB.

From these investigations it can be stated that the decomposition behaviour in highly concentrated solution, and naturally also in suspensions, resembles the decomposition mechanism in solid AB with respect to the importance of DADB.

These results have important implications for the development of possible high-capacity hydrogen-generation devices based on AB in organic solvents, since the dehydrogenation kinetics is one critical factor in the reactor design and layout in all conceivable applications.

Experimental Section

Materials: All experiments and measurements were performed under argon 5.0. AB was purchased from SAFC and purified by means of Soxhlet extraction with dry diethyl ether. Triglyme (2,5,8,11-tetraoxadodecane) was obtained from Aldrich (purity 98%) and distilled from sodium at 90 °C and 0.2 bar. DADB was synthesized according to literature methods[8] and characterized by XRD, and ^{11}B and ^{1}H NMR spectroscopy. The obtained product was >75% pure with AB as the only byproduct. CTB was synthesized as described in the literature[10] and was further purified by vacuum sublimation to result in a purity of 98% as demonstrated by ^{11}B and ^{1}H NMR spectra.

NMR Spectroscopy Sample Preparation: In a typical NMR-spectroscopy-monitored dehydrogenation experiment, triglyme (12–16 g) and an amount of AB, which varied from 0.07 g (0.1 м) to 2.75 g (6.0 м), were mixed in a two-necked Schlenk flask. For suspensions ($[AB]_0$ from 16 to 23 м) the amount of AB was fixed at 2.0 g. The flask was connected to a reflux condenser and a silicon oil trap. The hydrogen release of the samples was measured volumetrically. About 15–20 samples were dynamically taken during each dehydrogenation experiment. Samples were taken by using a metal-free syringe with a polytetrafluoroethylene (PTFE) needle to prevent catalytic effects. The samples were filled into NMR spectroscopy tubes and diluted with TG from the 1:2 to the 1:5 ratio (according to their original concentration) to reduce signal broadening.

Pressure Measurements: The above-described AB/TG mixtures (1–23 м, 0.3–3.0 g) were isothermally decomposed in a Schlenk flask at temperatures that ranged from 70 to 110 °C. The vessel was connected to a reflux condenser and a 2 L gas tank equipped with pressure and temperature sensors. The pressure and temperature of the gas tank were constantly monitored during the experiments.

^{11}B NMR Spectroscopic Measurements: All samples were measured with a Bruker DPX 400 spectrometer (7.06 T) operating at 400 MHz for ^{1}H and 128 MHz for ^{11}B. ^{11}B shifts were referenced externally to $BF_3{\cdot}Et_2O$ ($\delta = 0$ ppm).

Computation of Relative Peak Areas: Relative ^{11}B NMR spectroscopic peak areas were determined by fitting the corresponding peaks with the software PeakFit, which determined the value of their integrals and divided them by the ones of the complete spectrum (the latter representing the total boron content). The given error bars (when stated) reflect the influence of the integration borders of the signals in the case of overlapping peaks.

Acknowledgments

We thank the German Federal Ministry for the Environment, Nature Conservation and Nuclear Safety (BMU) for partly funding this work and the Bundesministerium für Bildung und Forschung for financial support of J. K. and F. B.

---

[1] J. Baumann, F. Baitalow, F. P. Hoffmann, *Thermochim. Acta* **2000**, *343*, 19.
[2] F. Baitalow, J. Baumann, G. Wolf, K. Jaenicke-Rossler, G. Leitner, *Thermochim. Acta* **2002**, *391*, 159.
[3] A. C. Stowe, W. J. Shaw, J. C. Linehan, B. Schmid, T. Autrey, *Phys. Chem. Chem. Phys.* **2007**, *9*, 1831.
[4] M. E. Bluhm, M. G. Bradley, R. Butterick III, U. Kusari, L. G. Sneddon, *J. Am. Chem. Soc.* **2006**, *128*, 7748.
[5] R. Schellenberg, J. Kriehme, G. Wolf, *Thermochim. Acta* **2007**, *457*, 103.
[6] W. J. Shaw, J. C. Linehan, N. K. Szymczak, D. J. Heldebrant, C. Yonker, D. M. Camaioni, R. T. Baker, T. Autrey, *Angew. Chem.* **2008**, *120*, 7603; *Angew. Chem. Int. Ed.* **2008**, *47*, 7493–7496.
[7] J. S. Wang, R. A. Geanagel, *Inorg. Chim. Acta* **1988**, *148*, 185.
[8] S. G. Shore, K. W. Böddeker, *Inorg. Chem.* **1964**, *3*, 914.
[9] D. F. Gaines, R. Schaeffer, *J. Am. Chem. Soc.* **1964**, *86*, 1505.
[10] G. H. Dahl, R. Schaeffer, *J. Am. Chem. Soc.* **1961**, *83*, 3032–3034.

Received: July 29, 2011